

## Article

# Physiological and Antioxidative Effects of Strontium Oxide Nanoparticles on Wheat

Mustafa Güven Kaysım<sup>1</sup>, Ahmet Metin Kumlay<sup>1</sup>, Kamil Haliloglu<sup>2</sup> , Aras Türkoğlu<sup>3,\*</sup> ,  
Magdalena Piekutowska<sup>4</sup> , Hayrunnisa Nadaroğlu<sup>5,6</sup> , Azize Alayli<sup>7</sup> and Gniewko Niedbala<sup>8,\*</sup> 

- <sup>1</sup> Department of Field Crops, Faculty of Agriculture, Iğdir University, Iğdir 76000, Türkiye; mguvenkaysim@gmail.com (M.G.K.); akumlay@hotmail.com (A.M.K.)
- <sup>2</sup> Department of Field Crops, Faculty of Agriculture, Ataturk University, Erzurum 25240, Türkiye; kamilh@atauni.edu.tr
- <sup>3</sup> Department of Field Crops, Faculty of Agriculture, Necmettin Erbakan University, Konya 42310, Türkiye
- <sup>4</sup> Department of Botany and Nature Protection, Institute of Biology, Pomeranian University in Słupsk, 22b Ar-ciszewskiego St., 76-200 Słupsk, Poland; magdalena.piekutowska@upsl.edu.pl
- <sup>5</sup> Department of Food Technology, Vocational College of Technical Sciences, Ataturk University, Erzurum 25240, Türkiye; hnisa25@atauni.edu.tr
- <sup>6</sup> Department of Nanoscience and Nano-Engineering, Institute of Science, Ataturk University, Erzurum 25240, Türkiye
- <sup>7</sup> Department of Nursing, Faculty of Health Sciences, Sakarya University of Applied Sciences, Sakarya 54187, Türkiye; aalayli@subu.edu.tr
- <sup>8</sup> Department of Biosystems Engineering, Faculty of Environmental and Mechanical Engineering, Poznań University of Life Sciences, Wojska Polskiego 50, 60-627 Poznań, Poland
- \* Correspondence: aras.turkoglu@erbakan.edu.tr (A.T.); gniewko.niedbala@up.poznan.pl (G.N.)

**Abstract:** We explored the impact of strontium oxide nanoparticles (SrO-NPs), synthesized through a green method, on seedling growth of bread wheat in hydroponic systems. The wheat plants were exposed to SrO-NPs concentrations ranging from 0.5 mM to 8.0 mM. Various parameters, including shoot length (cm), shoot fresh weight (g), root number, root length (cm), root fresh weight (g), chlorophyll value (SPAD), cell membrane damage (%), hydrogen peroxide (H<sub>2</sub>O<sub>2</sub>) value (μmol/g), malondialdehyde (MDA) value (ng/μL), and enzymatic activities like ascorbate peroxidase (APX) activity (EU/g FW), peroxidase (POD) activity (EU/g FW), and superoxide dismutase (SOD) activity (U/g FW), were measured to assess the effects of SrO-NPs on the wheat plants in hydroponic conditions. The results showed that the SrO-NPs in different concentrations were significantly affected considering all traits. The highest values were obtained from the shoot length (20.77 cm; 0.5 mM), shoot fresh weight (0.184 g; 1 mM), root number (5.39; 8 mM), root length (19.69 cm; 0 mM), root fresh weight (0.142 g; 1 mM), SPAD (33.20; 4 mM), cell membrane damage (58.86%; 4 mM), H<sub>2</sub>O<sub>2</sub> (829.95 μmol/g; 6 mM), MDA (0.66 ng/μL; 8 mM), APX (3.83 U/g FW; 6 mM), POD (70.27 U/g FW; 1.50 mM), and SOD (60.77 U/g FW; 8 mM). The data unequivocally supports the effectiveness of SrO-NPs application in promoting shoot and root development, chlorophyll levels, cellular tolerance, and the activation of enzymes in wheat plants.

**Keywords:** *Triticum aestivum* L.; hydroponic systems; green synthesis; antioxidative enzymes



**Citation:** Kaysım, M.G.; Kumlay, A.M.; Haliloglu, K.; Türkoğlu, A.; Piekutowska, M.; Nadaroğlu, H.; Alayli, A.; Niedbala, G. Physiological and Antioxidative Effects of Strontium Oxide Nanoparticles on Wheat. *Agronomy* **2024**, *14*, 770. <https://doi.org/10.3390/agronomy14040770>

Academic Editor: Prakash M Gopalakrishnan Nair

Received: 5 March 2024

Revised: 3 April 2024

Accepted: 5 April 2024

Published: 8 April 2024



**Copyright:** © 2024 by the authors. Licensee MDPI, Basel, Switzerland. This article is an open access article distributed under the terms and conditions of the Creative Commons Attribution (CC BY) license (<https://creativecommons.org/licenses/by/4.0/>).

## 1. Introduction

The bread wheat plant holds significant importance in human nutrition [1]. As one of the most extensively cultivated grains globally, it sustains approximately two-thirds of the world's population, boasting a production capacity of 670.8 million tons [2]. Wheat finds widespread use in the production of various food items, including bread, pasta, bulgur, noodles, cakes, and biscuits [3]. Not only do bread wheat plants offer high nutritional value, but they are also easily processed and highly adaptable. Due to its integration into the food chain, wheat serves as a prominent subject in biotechnological studies [4].

Metal ions play a pivotal role in biochemical processes crucial for plant development. However, when their concentration surpasses the optimal level within the plant, they exert negative effects on growth, both directly and indirectly. Exposure to high metal ion concentrations can lead to direct toxic effects, such as the inhibition of cytoplasmic enzymes and structural damage to cells due to oxidative stress [5]. Metal toxicity is recognized to harm plant cell membranes, impede transpiration, disrupt protein synthesis, impair photosynthesis, hinder the photosynthetic rate, and influence the activity of various enzymes [6]. Additionally, metals are known to interfere with chlorophyll synthesis either by directly inhibiting an enzymatic step or inducing a deficiency of essential nutrients [7].

To enhance productivity in the efficient use of resources, agriculture requires strengthening and revitalization through innovative, science-based technologies. Nanotechnology holds great promise in shaping a more sustainable future for agriculture [8]. Apart from their use in agriculture, NPs play a crucial role in smart release systems and real-time tracking systems. These NPs have been employed in studies to enhance efficiency while minimizing the entry of pesticides and herbicides. Furthermore, NPs find applications in groundwater and field purification efforts [9]. Numerous investigations have demonstrated that the application of different metal NPs at appropriate concentrations can have diverse positive effects on plants [10–13]. The extensively altered physiochemical properties of nanoparticles, attributed to their smaller size and larger surface area, contribute to their widespread application across various bioscience disciplines [14]. Nanoparticles, including gold (Au), silver (Ag), copper (Cu), zinc (Zn), aluminum (Al), silica (Si), zinc oxide (ZnO), cesium oxide (Ce<sub>2</sub>O<sub>3</sub>), titanium dioxide (TiO<sub>2</sub>), and magnetized iron (Fe), have been employed in agricultural applications [15].

While numerous studies have detailed the effects of nanoparticles (NPs) on plants, there remains some uncertainty concerning the toxicity and application of SrO-NPs, particularly in wheat-related scenarios. Strontium is a soft, silvery metallic element often found in rocks, soil, fossil fuel, water, and oil. Strontium (Symbol Sr, Atomic no. 38, atomic weight: 87.62 g/mol) is a naturally and widely occurring alkaline earth metal (group 2A, in period 5, between calcium and barium). The mineral was discovered by Adair Crawford and William Cruickshank in Strontian (Scotland) in 1790. Sr ore is generally found in nature in the form of minerals such as strontium sulfate (SrSO<sub>4</sub>) and strontianite (SrCO<sub>3</sub>); however, it can form a variety of compounds that may or may not be water-soluble. Sr in the atmosphere is in the form of fresh or dry aerosols. The main chemical species in air is strontium oxide (SrO). The chemical and biochemical behavior of radiostrontium and stable strontium is analogous in both soil solution and plants. Consequently, numerous experiments investigating the uptake and distribution of radiostrontium by plants have utilized stable strontium as a surrogate [16]. Regarding chemical toxicity, due to its chemical similarity, strontium displaces calcium (Ca) and induces calcium deficiency in organisms [17]. Brooks [18] assessed the toxicity level of strontium in plants to be 30 ppm. Subsequently, various model plants have been subjected to test studies to ascertain the toxicity and impacts of stable strontium in both hydroponic and soil cultures, with their overall conditions being observed [16,19]. It has been documented that strontium (Sr) exhibits both positive and negative effects on the growth, root development, shoots, and cell membranes of plants, contingent on the applied dosage [16]. However, the impact of strontium SrO-NPs on plants remains unknown. Additionally, no studies have examined SrO-NPs in wheat. This research investigated the effect of SrO-NPs in wheat for the first time. In this study, the effects of various concentrations of SrO-NPs in wheat including seedling growth, physiological parameters, and antioxidant analysis were investigated.

## 2. Materials and Methods

### 2.1. Plant Material

In this study, the Esperia bread wheat variety was employed. The wheat cultivar utilized was sourced from the Atatürk University Faculty of Agriculture, Department of Field Crops in Türkiye.

## 2.2. Preparation of Plant Extract

Plant extract preparation involved collecting walnut shells from Tortum/Erzurum, Turkey, with identification assistance from taxonomists. The walnut shells underwent multiple washes with distilled water to remove dust and soil. Subsequently, 25 g of small pieces were finely ground to create a uniform mixture in a blender with the addition of 250 mL of distilled water. The resulting mixture underwent centrifugation at  $5000 \times g$  for 10 min, and the obtained supernatant was utilized for the green synthesis process.

## 2.3. Green Synthesis and Characterization of SrO-NPs

Top of Form Green synthesis of SrO nanoparticles (NPs) was initiated using walnut shell extract, and the surface topography of the SrO-NPs was characterized through SEM. The surface morphologies were examined utilizing Metek, Apollo prime,  $10 \text{ mm}^2$  active area, S50 microscope inspect (FEI Company, Brno, Czech Republic), and R580 SE detector SEM operating at 20 kV, with energy-dispersive X-ray (EDAX) analysis attached to the scanning electron microscope (SEM). Subsequently, XRD analysis was conducted to ascertain the crystallinity of the SrO-NPs. X-ray diffraction (XRD) patterns were obtained on a PANalytical EMPYREAN XRD (Malvern Panalytical Inc., Westborough, MA, USA) instrument equipped with Ni-filtered Cu K $\alpha$  radiation ( $\lambda = 0.1542 \text{ nm}$ ) in the range of  $10\text{--}80^\circ$  at a scanning rate of  $4^\circ \text{ min}^{-1}$ . Furthermore, FT-IR analysis of the SrO-NPs was performed using a Vertex 80 Model FT-IR Frontier spectrophotometer (Bruker Ltd., Karlsruhe, Germany) with the attenuated total reflection (ATR) technique in the  $4000\text{--}400 \text{ cm}^{-1}$  region [20].

## 2.4. Application of SrO-NPs on Wheat and Their Growing Condition

In this study, SrO-NPs synthesized through a green synthesis method were administered to plants at varying concentrations (0, 0.5 mM, 1 mM, 1.5 mM, 2 mM, 4 mM, 6 mM, and 8 mM). Approximately 300  $\mu\text{L}$  of plant extract from walnut shell was added to a sample containing SrCl $_2$  solution (10 mL, 10 mM) and left to incubate for 4 h. A noticeable transformation occurred as the solution transitioned to a light-yellow hue, suggestive of the formation of SrO-NPs [21,22]. Wheat seeds underwent sterilization using a solution composed of 70% ethyl alcohol and 30% sodium hypochlorite, followed by thorough rinsing with pure water. Seeds reaching a length of 2 cm after a 3-day pre-germination period at an ambient temperature of  $25^\circ\text{C}$  were then transferred to the hydroponic system. A stock solution, derived from the Hoagland and Arnon [23] formulation, was prepared. SrO-NPs were subsequently added at concentrations ranging from 0 to 8 mM, with the pH adjusted to 5.8. Randomized plots were established with four replications based on the experimental design. Subsequently, 250 mL of the prepared solution was added to each replicate group, and five germinated seeds were planted. The hydroponic system was operated at  $25 \pm 1^\circ\text{C}$  under an 18 h light/6 h dark photoperiod, with a photon density of  $120 \mu\text{mol photon/m}^2\text{s}$ . The experiment concluded at the end of the 7th day.

## 2.5. Measuring the Chlorophyll Value

The chlorophyll value of the plants was measured at the conclusion of the application. The average values were obtained by measuring each sample in the repetition using the SPAD-502 Plus (Konica Minolta Optics, Tokyo, Japan) device, selected from the flag leaves of the plant. The measurement method adhered to the procedure outlined by Nezami et al. [24].

## 2.6. Morphological Observations

Upon completion of the application, morphological observations were conducted. The shoot and root lengths of the plants were measured using a millimeter scale (cm), while the shoot and root weights were determined with a precision scale (g). Additionally, the number of roots was quantified through counting.

### 2.7. Cell Membrane Damage

Cell membrane damage at the conclusion of the application was assessed using an EC meter (Thermo Fisher Scientific, Waltham, MA, USA), following the method outlined by Lutts [25]. Leaf samples weighing a total of 100 mg were obtained from each experimental group, washed with pure water, and placed in Falcon tubes containing 15 mL of pure water. The tubes were maintained at 25 °C for 24 h. After this incubation period, samples with recorded electrical conductivity (EC1) values were autoclaved at 120 °C for 20 min. Subsequently, the samples were cooled to 25 °C, and the electrical conductivity (EC2) values were determined through another measurement with an EC meter. Cell membrane damage was calculated by the following formula:

$$\text{Cell membrane damage} = \frac{EC1}{EC2} \times 100 \quad (1)$$

### 2.8. H<sub>2</sub>O<sub>2</sub>, MDA, and Stress Enzyme Analysis

At the conclusion of the application, the examination of H<sub>2</sub>O<sub>2</sub> and MDA values followed the procedures outlined by Tiryaki et al. [26]. Furthermore, the activities of stress enzymes, including SOD, POD, and APX, were analyzed through absorbance measurements using microplate reader (Multiskan GO, Thermo Scientific, Hudson, NH, USA). The activity of the SOD enzyme was determined by monitoring the inhibition of the photoreaction of NBT. Each sample was loaded into the wells of a spectrophotometer plate with 20 µL of sample, 170 µL of SOD assay buffer, and 10 µL of riboflavin solution for each replicate. The blank well was loaded with 190 µL of SOD assay buffer and 10 µL of riboflavin solution. The prepared plate was incubated under fluorescent light for 10 min to initiate color development of NBT. At the end of this period, the plate was placed into the spectrophotometer device, and measurements were taken at a wavelength of 560 nm to record the results. One unit of SOD activity was defined as the enzyme amount causing 50% inhibition of NBT reduction, and the results are expressed as U/g leaf. For POD analysis, each sample was loaded into the wells of the spectrophotometer plate for a single replicate with 5 µL of sample and 245 µL of POD assay buffer. The prepared plate was then placed into the spectrophotometer device, absorbance measurements were taken at a wavelength of 470 nm for 1 min with intervals of 15 s, and the results were recorded. At 25 °C, the enzyme amount causing an increase of 0.01 in absorbance within 1 min was considered as 1 enzyme unit, and the results are expressed as enzyme units per gram of leaf (U/g leaf). For APX analysis, each sample was loaded into the wells of the spectrophotometer plate for a single replicate with 20 µL of sample and 180 µL of APX assay buffer. The prepared plate was then placed into the spectrophotometer device, and measurements were taken at 290 nm wavelength for 3 min with intervals of 30 s after 1 s of pre-shaking. The results are recorded as enzyme units per gram of fresh leaf (U/g leaf) [27].

### 2.9. Data Analysis

The study of different concentrations (0, 0.5 mM, 1 mM, 1.5 mM, 2 mM, 4 mM, 6 mM, and 8 mM) of SrO-NPs was applied based on a completely randomized design with four replications. Analysis of variance (ANOVA) was performed using the general linear model procedure in JMP statistical software (JMP, Version 15th edition. SAS Institute Inc., Cary, NC). The mean values obtained from the treatments were compared using the least-significant difference test (LSD) with a significance level set at  $\alpha = 0.05$ .

## 3. Results and Discussion

### 3.1. Synthesis and Characterization of SrO-NPs

In this study, we successfully synthesized SrO-NPs utilizing walnut shell extract as a green and sustainable reducing and stabilizing agent. The synthesis process was conducted via a facile and eco-friendly method, aiming for the development of environmentally benign nanoparticle synthesis techniques. The characterization of the synthesized SrO-

NPs was conducted using various analytical techniques to understand their structural, morphological, and chemical properties. The following results were obtained.

### 3.1.1. SEM Analysis

The chemical and mineralogical compositions of the synthesized green zinc NPs were determined by scanning electron microscopy (SEM), which was used to examine the surface of the adsorbent. Images of the SrO-NPs were taken at 29.43 K $\times$  magnification by a Zeiss instrument (Zeiss, Oberkochen, Germany), and the active area was 10 mm<sup>2</sup> (Figure 1A). The energy-dispersive X-ray (EDX) analysis was conducted to determine the elemental composition of the synthesized SrO-NPs. The results confirmed the presence of strontium (Sr) and oxygen (O) elements, consistent with the expected composition of SrO. The spectrum displayed distinct peaks corresponding to the characteristic X-ray emissions of strontium and oxygen, indicating the successful formation of SrO nanoparticles without any detectable impurities. The elemental composition analysis corroborates the purity of the synthesized nanoparticles (Figure 1B).

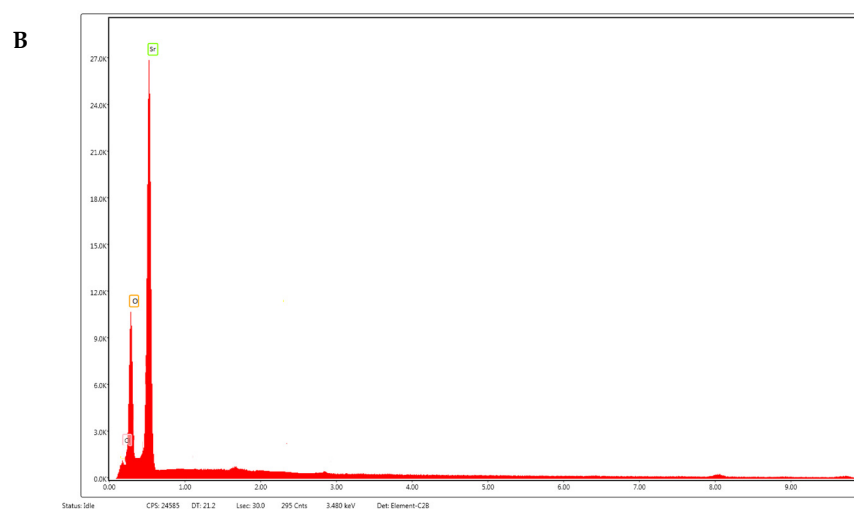
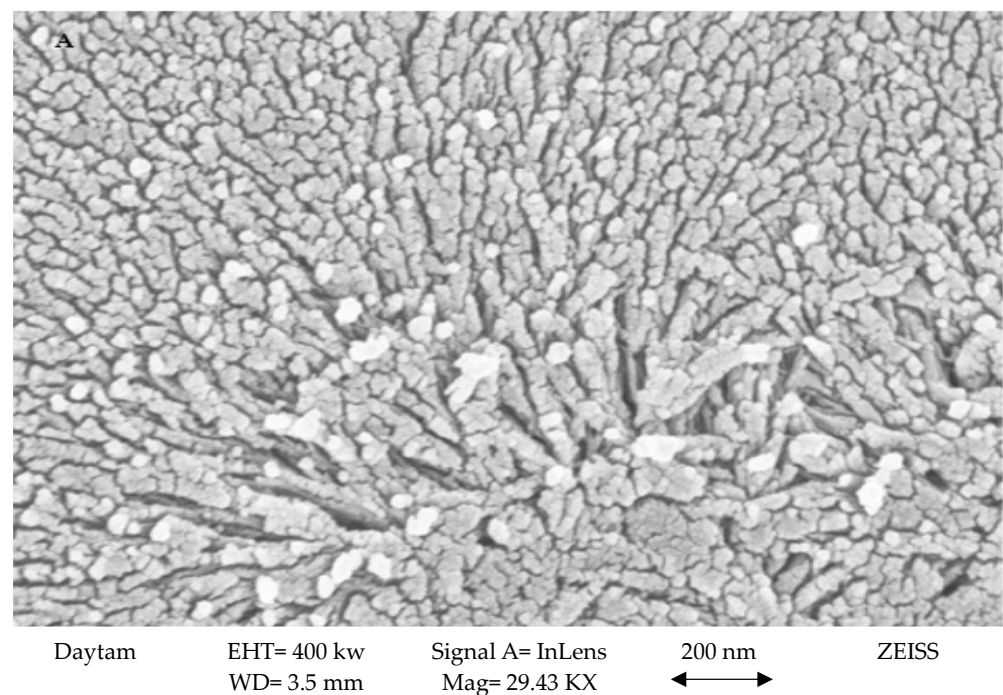


**Figure 1.** (A) SEM analysis result of the SrO with 29.43 K $\times$  magnification, (B) EDX analysis result of the SrO-GO.

### 3.1.2. XRD of ZnO-NPs

The description of the XRD pattern and crystallographic analysis of SrO-NPs synthesized using a peroxidase enzyme catalyst is clear and informative. The identification of characteristic peaks at specific  $2\theta$  values corresponding to (111), (130), (220), and (222) planes provide valuable information about the crystal structure (Figure 2). Additionally, referencing a previously reported XRD pattern by Apsana et al. [28] adds context and contributes to the existing knowledge in the field of SrO synthesis. The peak observed along the (111) plane signifies the presence of well-defined crystalline domains within the SrO-NPs. This peak represents the most densely packed lattice planes in the crystal structure, indicating a high degree of structural order. The prominence of the (111) peak suggests the formation of crystallites with a preferred orientation along this plane, highlighting the uniformity and quality of the crystal lattice. Additionally, the peak corresponding to the (130) plane indicates an additional crystallographic orientation within the SrO-NPs. This observation underscores the complexity of the crystal structure, with multiple orientations contributing to the overall arrangement of atoms. The presence of the (130) peak contributes significantly to the comprehensive structural analysis, providing further insights into the atomic arrangement and symmetry within the crystal lattice. Furthermore, the peak observed along the (220) plane serves as confirmation of the crystalline phase of the SrO-NPs. This peak provides crucial information regarding the crystal structure and symmetry of the nanoparticles, further validating their crystalline nature. The intensity and position of the (220) peak offers valuable clues about the crystallite size, lattice spacing, and overall crystallographic quality of the synthesized nanoparticles.

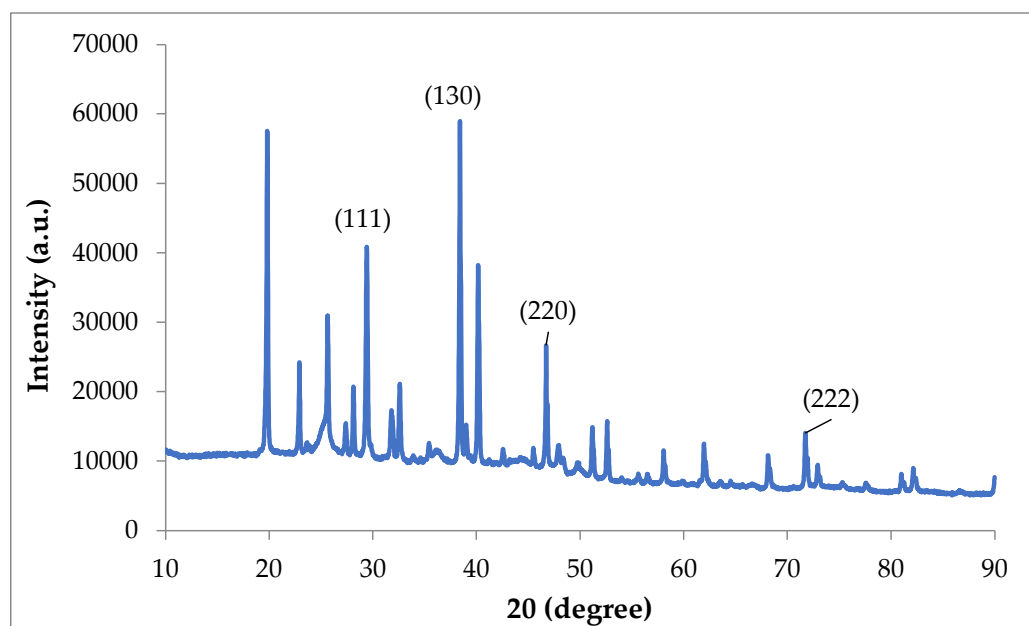


**Figure 2.** X-ray diffraction pattern of strontium oxide nanoparticles.

### 3.1.3. Fourier-Transform Infrared Spectroscopy (FTIR) Analysis

Our description of the FTIR spectrum for SrO-NPs is thorough and well structured. The assignment of peaks at specific wavenumbers to bending vibrations of Sr-O, as well as the identification of absorption bands related to OH and CO bonds, provides a comprehensive analysis (Figure 3). Referencing relevant studies by Nadaroglu et al. [22], Apsana et al. [29], and Alavi and Morsali [30] strengthens the interpretation of the FTIR results and places our findings within the literature.

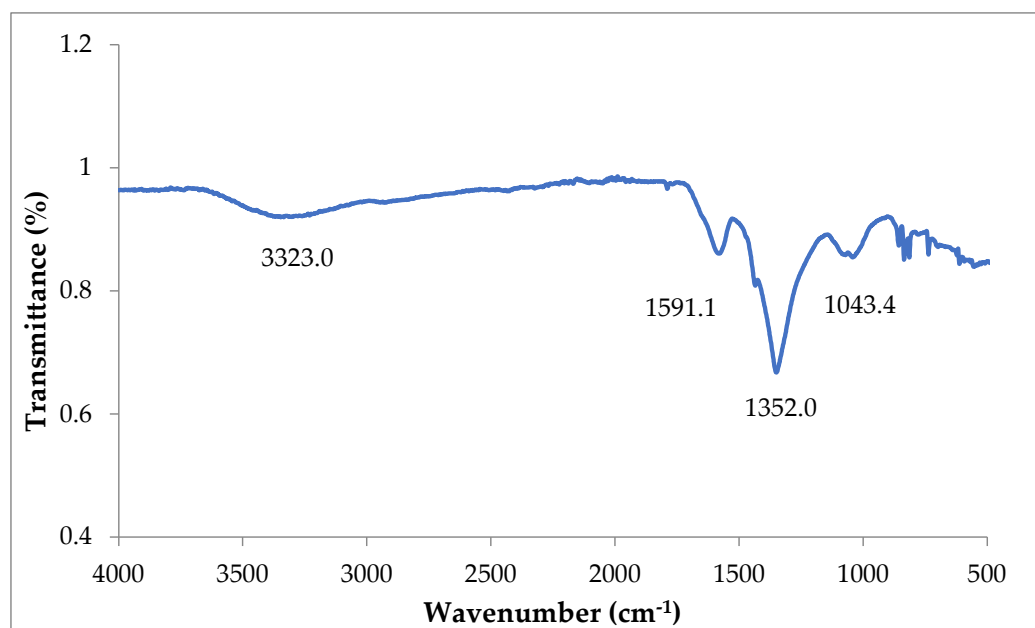


**Figure 3.** Fourier-transform infrared spectrum of strontium oxide nanoparticles.

### 3.2. Physiological Effect on Wheat of SrO-NPs

#### 3.2.1. Shoot Length

The shoot length results for wheat treated with SrO-NPs are illustrated in Figure 4A. The variance analysis results showed that for shoot length in wheat, a statistically significant difference among the treatments was observed ( $p < 0.001$ ). The 0.5 mM SrO-NPs treatment group exhibited the longest shoot length (20.78 cm), followed by the 1.0 mM SrO-NPs treatment group (20.31 cm) and the control group (20.07 cm). Conversely, the shortest shoots were obtained from the 8.0 mM SrO-NPs (15.84 cm) and 4.0 mM SrO-NPs treatments (16.12 cm). The initial increase in shoot lengths compared to the control was observed at lower SrO-NPs concentrations, but at higher concentrations, a significant decrease in shoot length occurred. These findings align with a study by Lee et al. [31], where Cu-NPs application similarly reduced the shoot length of wheat plants compared to the control group.

#### 3.2.2. Shoot Fresh Weight

From the analysis of variance results of shoot fresh weight, a statistically significant difference among the applications was identified ( $p < 0.001$ ) (Figure 4B). The heaviest fresh shoot weight was observed in the 0.5 mM SrO-NPs (0.1841 g) and 1.0 mM SrO-NPs (0.1842 g) treatments, followed by the 1.5 mM SrO-NPs treatment (0.1785 g). Conversely, the lowest shoot fresh weight was recorded with 8.0 mM SrO-NPs application (0.1351 g). The overall trend suggests that the shoot fresh weight decreased with increasing concentration, excluding the control and 6.0 mM SrO-NPs treatments. The findings of these results agree with Dimkpa et al. [32] on CuO and ZnO-NPs, Wang et al. (2014) on Ag-NPs, and Jiang et al. [33] on TiO<sub>2</sub>-NPs. The application of TiO<sub>2</sub> has been shown to decrease the fresh weight of wheat plant shoots in a dose-dependent manner.

#### 3.2.3. Number of Roots

Variance analysis of root number showed a highly significant difference among the concentrations ( $p < 0.001$ ) (Figure 4C). The highest number of roots was observed after applying 8.0 mM SrO-NPs (5.39), followed by 1.0 mM SrO-NPs (4.85), 6.0 mM SrO-NPs (4.83), and 4.0 mM SrO-NPs (4.83). The control group exhibited the lowest number of roots (4.55). This situation causes an increase in the number of roots as the SrO-NPs concentration increases. Supporting this observation, Iqbal et al. [34] reported an increase in the number of roots in their study with AgNO<sub>3</sub>-NPs application, indicating consistency with our findings.

### 3.2.4. Root Length

Statistically significant differences were observed among the concentrations of this study ( $p < 0.001$ ) (Figure 4D). Notably, SrO-NPs treatments were found to increase concentration and lead to decrease in root length. The control treatment exhibited the longest roots (19.69 cm), followed by the 0.5 mM SrO-NPs treatment (18.12 cm). In contrast, the shortest roots were observed in 8.0 mM SrO-NPs (6.03 cm) and 4.0 mM SrO-NPs (6.47 cm). This suggests that SrO-NPs contribute to the reduction in root length, which is a favorable characteristic for transferring plants obtained from tissue culture media to pots and greenhouses, facilitating their establishment in the soil. These findings align with the results of Rafique et al. [35] and Jiang et al. [33], where the application of TiO<sub>2</sub>-NPs led to similar effects. Additionally, McManus et al. [36] reported that CuO-NPs application reduced the length of roots in wheat plants, supporting the outcomes observed in our study.

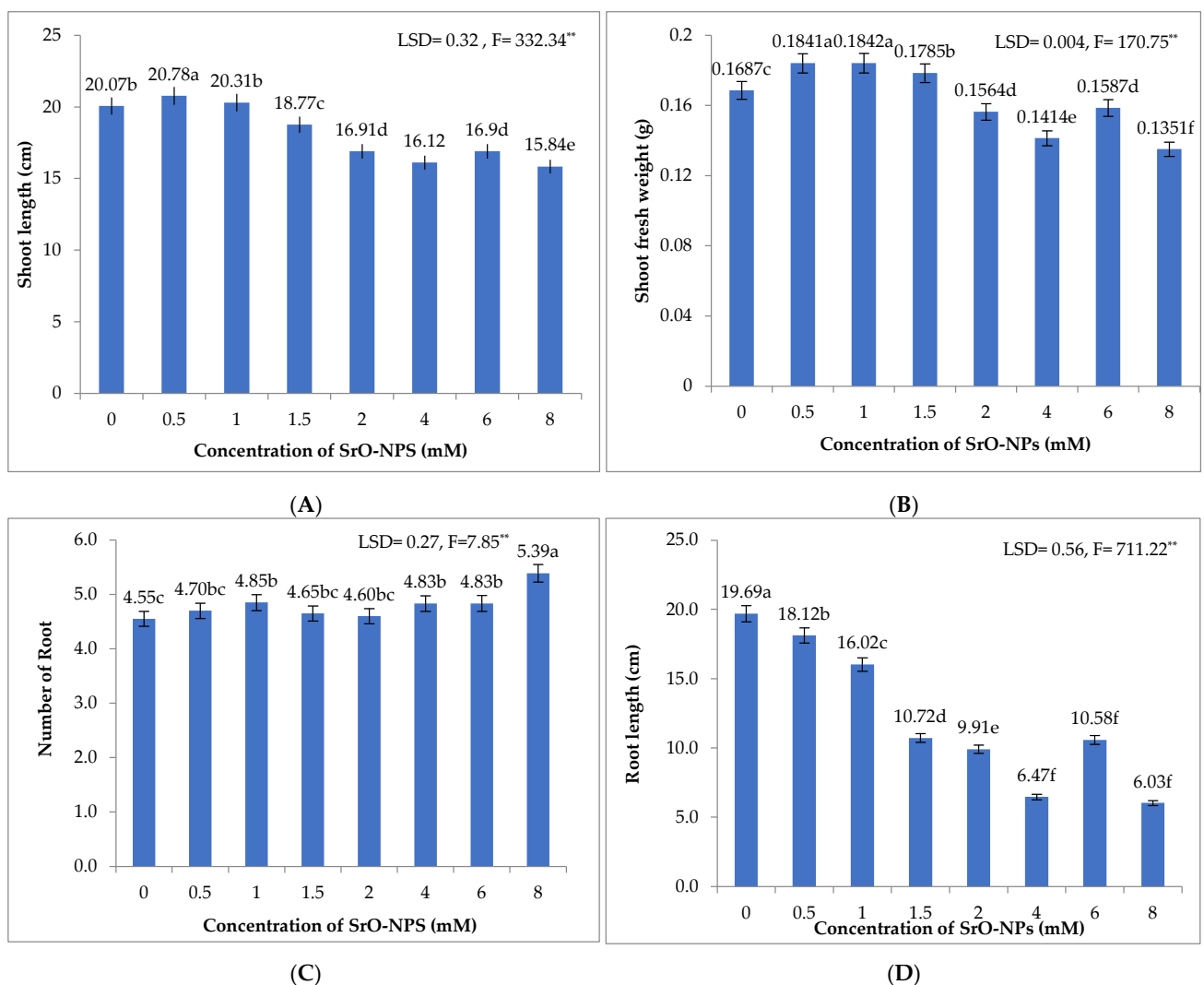
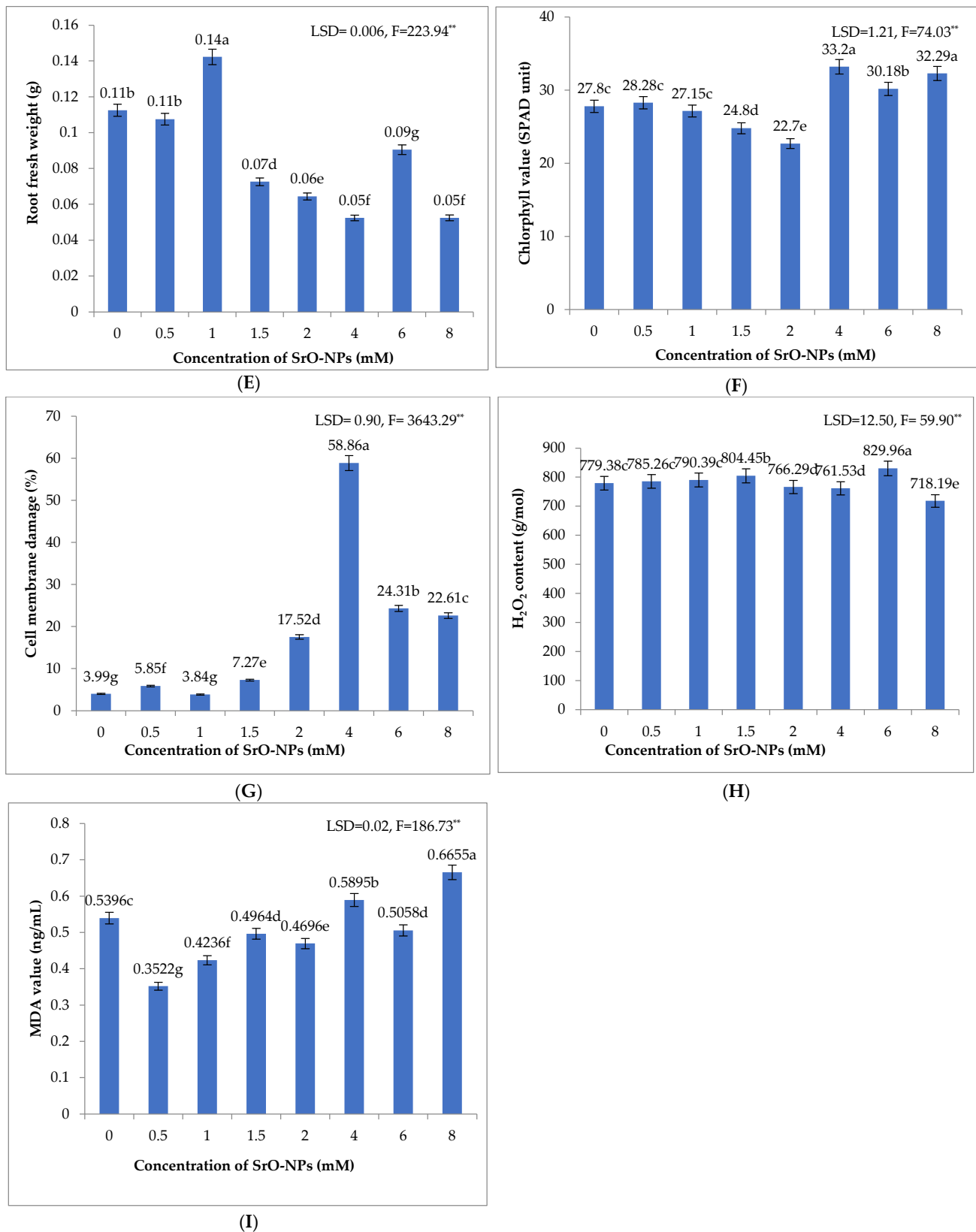


Figure 4. Cont.



**Figure 4.** Effects of different concentrations of SrO-NPs on wheat plant: (A) shoot length (cm), (B) shoot fresh weight (g), (C) number of roots, (D) root length (cm), (E) fresh root weight (g), (F) chlorophyll value (SPAD), (G) cell membrane damage (%), (H) H<sub>2</sub>O<sub>2</sub> value (μmol/g), and (I) MDA value (ng/μL). Different lowercase letters indicate non-significant differences between each item. F values marked with \*\* is significant at the probability level of 0.01.

### 3.2.5. Fresh Root Weight

From the variance analysis results for fresh root weight, a statistically significant difference among the concentration was identified ( $p < 0.001$ ) (Figure 4E). The highest fresh root weight was observed in the 1.0 mM SrO-NPs treatment (0.14 g), followed by the control (0.11 g) and the 0.5 mM SrO-NPs treatment (0.11 g). Conversely, the lowest fresh root weight was recorded after applying 4.0 mM SrO-NPs (0.05 g) and 8.0 mM SrO-NPs (0.053 g). Despite the non-linearity in root age weights, there is an overall decrease, which is considered desirable for the acclimation of plantlets from tissue culture media to soil. These results align with the findings of Lee et al. [31], who studied Cu-NPs application, with those of Mahmoodzadeh et al. [37], who investigated TiO<sub>2</sub>-NPs application, and with those of McManus et al. [36], who reported that CuO-NPs application decreases the age and weight of roots in wheat plants.

### 3.2.6. Chlorophyll Value

Stress factors can induce a decline in chlorophyll synthesis in plants, with metal stress inhibiting protochlorophyll reductase and aminolevulinic acid synthesis, resulting in the generation of free radicals and oxidative breakdown of thylakoid membrane lipids [38]. The impact of stress on plants can be assessed by quantifying chlorophyll levels. Variance analysis of the chlorophyll value treated with SrO-NPs revealed a statistically significant difference among the treatments ( $p < 0.001$ ) (Figure 4F). Notably, the effects of applying 4 mM SrO-NPs (33.20) and 8.0 mM SrO-NPs (32.29) were comparable to the control (27.80), while a reduction in chlorophyll value occurred at 1.5 and 2.0 mM SrO (24.80 and 22.70, respectively). Conversely, applications of 4.0 mM (33.20), 6.0 mM (30.18), and 8.0 mM (32.29) SrO-NPs appeared to enhance the chlorophyll value compared to the control group. The positive reaction between the chlorophyll value and SrO-NPs concentration suggests a potential increase in photosynthesis, contributing positively to plant growth and development. In conclusion, our findings support the notion that SrO-NPs application positively influences chlorophyll levels in wheat plants. This aligns with similar studies where Dimkpa et al. [39] utilized ZnO-NPs, Ali et al. [40] employed Si (silicon) NPs, and Hussain et al. [41] applied FeO-NPs, all resulting in increased chlorophyll values in wheat plants.

### 3.2.7. Cell Membrane Damage

The impact of stress factors on plant cell membrane permeability, fluidity, and protein activity, leading to increased electrical conductivity, is a well-established phenomenon. The examination of electrical conductivity is a reliable method for detecting cell membrane damage, a key parameter in assessing the effects of stress [42]. For the variance analysis results of cell damage, a highly significant difference among the applications was observed ( $p < 0.001$ ) (Figure 4G). The highest value of cell membrane damage occurred in the 4.0 mM SrO-NPs treatment (58.86%), followed by the 6.0 mM SrO-NPs treatment group (24.31%). In contrast, the lowest cell membrane damage was observed in the 1.0 mM SrO-NPs treatment (3.84%) and the control treatment (3.99%). This aligns with the study by Gao et al. [43], where GO-NPs application to rice plants was investigated, and with the findings of Iftikhar et al. [44] who reported increased cell membrane damage in wheat plants following ZnO-NPs application.

### 3.2.8. H<sub>2</sub>O<sub>2</sub> Value

The synthesis of H<sub>2</sub>O<sub>2</sub> by the SOD enzyme, leading to potential lipid peroxidation and cell membrane damage, is a recognized process in response to stress. The detoxification of H<sub>2</sub>O<sub>2</sub> occurs through antioxidative enzymes such as POD, APX, and CAT. Monitoring the value of H<sub>2</sub>O<sub>2</sub> serves as a valuable measure to assess the degree of stress [45]. From the variance analysis results of H<sub>2</sub>O<sub>2</sub>, a statistically highly significant difference among the applications was observed ( $p < 0.001$ ), as depicted in Figure 4H. The highest value of H<sub>2</sub>O<sub>2</sub> was recorded after applying 6.0 mM SrO-NPs (829.96 µmol/g), followed by the 1.5 mM SrO-NPs treatment (804.45 µmol/g). Conversely, the lowest value of H<sub>2</sub>O<sub>2</sub> was obtained

from the 8.0 mM SrO-NPs treatment (718.19  $\mu\text{mol/g}$ ). This observation is consistent with the findings of Kheiri et al. [46] on Cs-NPs, with those of Rafique et al. [47] on TiO<sub>2</sub>-NPs, with those of Iftikhar et al. [44] on ZnO-NPs, and with those of Saleh et al. [48] on the application of NiO, all reporting an increase in the value of H<sub>2</sub>O<sub>2</sub> in wheat plants due to nanoparticle applications.

### 3.2.9. MDA Value

The occurrence of lipid peroxidation in the cell membrane results in the production of MDA, which, in turn, impairs the stability of the cell membrane. Therefore, MDA is considered an effective measure for determining the extent of oxidative damage in living organisms [49]. From the variance analysis results of MDA, a highly statistically significant difference among the concentration was observed ( $p < 0.001$ ) (Figure 4I). The greatest effect on MDA value was observed with 8.0 mM SrO-NPs (0.67 ng/ $\mu\text{L}$ ), followed by 4.0 mM SrO-NPs (0.59 ng/ $\mu\text{L}$ ). In contrast, the lowest MDA value was recorded in the 0.5 mM SrO-NPs treatment group (0.35 ng/ $\mu\text{L}$ ). Similar findings were found in previous studies where Da Costa and Sharma [50] reported increased MDA values in rice plants due to CuO-NPs application, García-Gómez et al. [51] noted an increased MDA value in corn plants following ZnO-NPs application, and Iftikhar et al. [44] reported elevated MDA values in wheat plants with ZnO-NPs application.

### 3.3. Antioxidant Effect on Wheat of SrO-NPs

APX, POD, and SOD serve as antioxidative enzymes crucial for shielding plants against stress conditions. The APX enzyme family, recognized as enzymatic antioxidants, is presumed to play a role in eliminating reactive oxygen derivatives encountered during plant stress, thereby safeguarding various cellular structures such as DNA, proteins, and lipids. The elevation in APX activity is believed to correlate with the mitigation or elimination of negative effects induced by plant stress [52]. POD, an antioxidant enzyme, effectively manages and detoxifies reactive oxygen derivatives, contributing to plant survival amidst stressful conditions [52]. Monitoring POD activity stands as a vital parameter for acquiring information regarding the impact of stress. SODs, characterized by their high catalytic activity, are enzymes responsible for converting the superoxide anion (O<sup>-2</sup>) into H<sub>2</sub>O<sub>2</sub>, a reactive oxygen derivative known to inflict damage on the plant's DNA, proteins, and lipids. An augmentation in SOD activity aids plants in withstanding both biotic and abiotic stress factors, facilitating their survival [53]. From the variance analysis results of APX, POD, and SOD enzyme activity, a statistically significant difference among the applications was identified ( $p < 0.001$ ) (Figure 5). The highest APX activity was recorded after the application of 6.0 mM SrO-NPs (3.84 U/g FW), followed by 4.0 mM SrO-NP (3.31 U/g FW) and 1.5 mM SrO-NP (3.47 U/g FW) applications. In contrast, the lowest APX activity was observed in the 0.5 mM SrO-NP treatment group (1.73 U/g FW). This increase in APX activity, which is crucial for removing reactive oxygen derivatives that damage DNA, proteins, and lipid structures in cells, indicates that SrO-NPs have a positive effect on the plants' antioxidative defense mechanisms.

In Figure 5, the highest POD activity was observed following the application of 1.5 mM SrO-NPs (70.28 EU/g FW), succeeded by 4.0 mM SrO-NP application (59.07 EU/g FW). Conversely, the lowest POD activity was recorded after applying 1.0 mM SrO-NPs (46.33 EU/g FW), 8.0 mM SrO-NPs (46.67 EU/g FW), and 0.5 mM SrO-NPs (46.98 EU/g FW).

Furthermore, Figure 5 reveals that the greatest SOD activity was obtained with 8.0 mM SrO-NP application (60.775 EU/g FW), followed by 4.0 mM SrO-NP (58.75 EU/g FW) and 6.0 mM SrO-NP (56.32 EU/g FW) applications. In contrast, the lowest SOD activity was detected in the 1.0 mM SrO-NP treatment group (43.14 EU/g FW) and the control treatment (43.496 EU/g FW). Comparatively, all SrO-NP treatments increased SOD activity in plant cells significantly, enhancing the plant defense mechanism compared to the control treatment (43.496 EU/g FW). The observed increase in POD, another crucial antioxidant

enzyme essential for plant survival under stress, suggests that NP application, especially up to a 2.0 mM dose, does not have drawbacks and may even have positive effects. This aligns with similar findings by Chen et al. [49], who reported that ZnO-NP application reduced POD levels in rice plants. Conversely, studies by Du et al. [54] for CeO<sub>2</sub>-NP application, Ali et al. [40] for Si-NP application, Du et al. [54] for ZnO-NP application, Hussain et al. [41] for FeO-NP application, and Jhazab et al. [55] reported results like ours, indicating that Ag-NP application increased SOD levels in wheat plants.

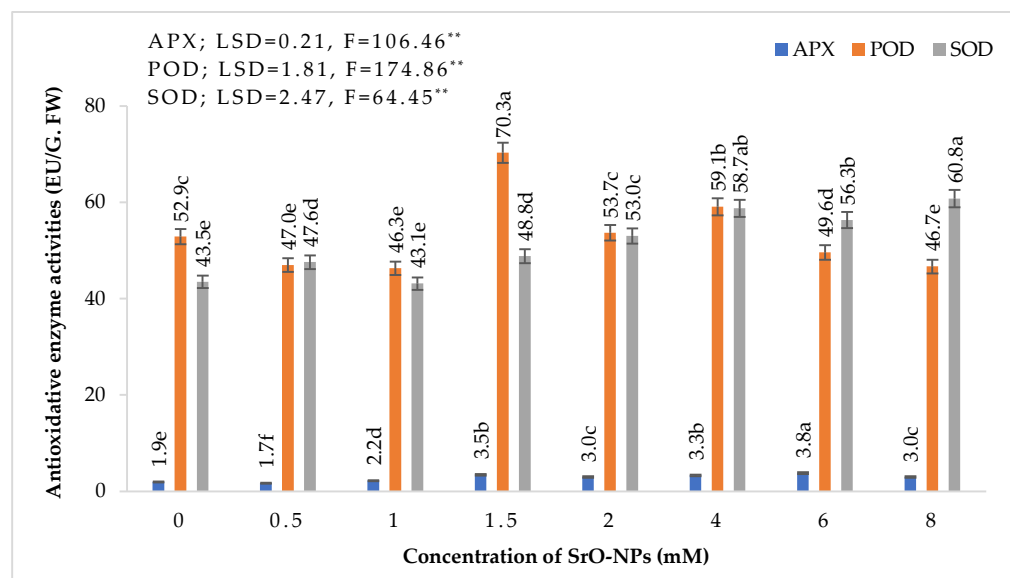


**Figure 5.** Effects of different concentrations of SrO-NPs on APX, POD, and SOD antioxidative enzyme activities (EU/g FW). Different lowercase letters indicate non-significant differences between each item. F values marked with \*\* is significant at the probability level of 0.01.

#### 4. Conclusions

Nanotechnology is widely used in several branches of science to improve the quality of life. The application of nanoparticles is continuously increasing in numerous fields including agriculture. Among the nanoparticles, metallic nanoparticles have gained significant interest in the past few years due to their unique physical and chemical characteristics. In recent times, there has been a surge in interest surrounding strontium oxide nanoparticles (SrO-NPs) due to their promising features and potential applications. The results obtained from the evaluation of all parameters indicate that SrO-NPs application in the concentration range of 0.0–1.5 mM positively impacted the Esperia wheat plant variety. The effectiveness of SrO-NP application was particularly notable within this concentration range. It is suggested that conducting studies at a more sensitive concentration, up to 1.5 mM, and exploring lower concentrations may yield more precise results for determining the optimum SrO-NP concentration. To enhance the efficient utilization of plant nutrients in hydroponic systems, greenhouses, and field settings, further investigations into the use of SrO-NPs in nanofertilizers or other innovative methods could contribute to researchers obtaining longer and heavier shoots, improving resistance to both biotic and abiotic stress factors.

**Author Contributions:** Conceptualization, M.G.K., A.M.K., K.H., A.T., H.N., A.A. and G.N.; methodology, M.G.K., A.M.K., K.H., A.T., M.P., H.N., A.A. and G.N.; software, M.G.K., A.M.K., K.H., A.T., M.P., H.N., A.A. and G.N.; validation, M.G.K., A.M.K., K.H., A.T., M.P., H.N., A.A. and G.N.; formal analysis, M.G.K., A.M.K., K.H., A.T., M.P., H.N., A.A. and G.N.; investigation, M.G.K., A.M.K., K.H., A.T., M.P., H.N., A.A. and G.N.; resources, M.G.K., A.M.K., K.H., A.T., H.N., A.A. and G.N.; data curation, M.G.K., A.M.K., K.H., A.T., M.P., H.N., A.A. and G.N.; writing—original draft preparation, M.G.K., K.H., A.T., M.P. and G.N.; writing—review and editing, M.G.K., A.M.K., K.H., A.T., M.P., H.N., A.A. and G.N.; visualization, M.G.K., A.M.K., K.H., A.T., H.N., A.A. and G.N., supervision,

A.M.K. and G.N.; project administration, A.M.K. and K.H.; funding acquisition, A.M.K. and K.H. All authors have read and agreed to the published version of the manuscript.

**Funding:** This research received no external funding.

**Data Availability Statement:** All data supporting the conclusions of this article are included in this article.

**Conflicts of Interest:** The authors claim no conflicts of interest in this work.

## References

- Moshawih, S.; Abdullah Juperi, R.a.N.A.; Paneerselvam, G.S.; Ming, L.C.; Liew, K.B.; Goh, B.H.; Al-Worafi, Y.M.; Choo, C.-Y.; Thuraisingam, S.; Goh, H.P. General health benefits and pharmacological activities of *Triticum aestivum* L. *Molecules* **2022**, *27*, 1948. [[CrossRef](#)] [[PubMed](#)]
- Shahzad, A.; Iqbal, M.; Asif, M.; Hirani, A.H.; Goyal, A. Growing wheat on saline lands: Can a dream come true? *Aust. J. Crop Sci.* **2013**, *7*, 515–524.
- Uthayakumaran, S.; Wrigley, C. Wheat: Grain-quality characteristics and management of quality requirements. In *Cereal Grains*; Elsevier: Amsterdam, The Netherlands, 2017; pp. 91–134.
- Delporte, F.; Mostade, O.; Jacquemin, J. Plant regeneration through callus initiation from thin mature embryo fragments of wheat. *Plant Cell Tissue Organ Cult.* **2001**, *67*, 73–80. [[CrossRef](#)]
- Jadia, C.D.; Fulekar, M. Phytoremediation of heavy metals: Recent techniques. *Afr. J. Biotechnol.* **2009**, *8*, 921–928.
- John, R.; Ahmad, P.; Gadgil, K.; Sharma, S. Heavy metal toxicity: Effect on plant growth, biochemical parameters, and metal accumulation by *Brassica juncea* L. *Int. J. Plant Prod.* **2009**, *3*, 65–76.
- Van Hoeck, A.; Horemans, N.; Van Hees, M.; Nauts, R.; Knapen, D.; Vandenhove, H.; Blust, R.  $\beta$ -Radiation stress responses on growth and antioxidative defense system in plants: A study with strontium-90 in *Lemna minor*. *Int. J. Mol. Sci.* **2015**, *16*, 15309–15327. [[CrossRef](#)] [[PubMed](#)]
- Zain, M.; Ma, H.; Chaudhary, S.; Nuruzaman, M.; Azeem, I.; Mehmood, F.; Rahman, S.U.; Aiwang, D.; Sun, C. Nanotechnology in precision agriculture: Advancing towards sustainable crop production. *Plant Physiol. Biochem.* **2023**, *206*, 108244. [[CrossRef](#)]
- Singh, H.; Sharma, A.; Bhardwaj, S.K.; Arya, S.K.; Bhardwaj, N.; Khatrı, M. Recent advances in the applications of nano-agrochemicals for sustainable agricultural development. *Environ. Sci. Process. Impacts* **2021**, *23*, 213–239. [[CrossRef](#)]
- Haliloğlu, K.; Türkoğlu, A.; Balpınar, Ö.; Nadaroğlu, H.; Alaylı, A.; Poczai, P. Effects of Zinc, Copper and Iron Oxide Nanoparticles on Induced DNA Methylation, Genomic Instability and LTR Retrotransposon Polymorphism in Wheat (*Triticum aestivum* L.). *Plants* **2022**, *11*, 2193. [[CrossRef](#)]
- Koçak, R.; Okcu, M.; Haliloğlu, K.; Türkoğlu, A.; Pour-Aboughadareh, A.; Jamshidi, B.; Janda, T.; Alaylı, A.; Nadaroğlu, H. Magnesium Oxide Nanoparticles: An Influential Element in Cowpea (*Vigna unguiculata* L. Walp) Tissue Culture. *Agronomy* **2023**, *13*, 1646. [[CrossRef](#)]
- Nalci, O.B.; Nadaroglu, H.; Pour, A.H.; Gungor, A.A.; Haliloglu, K. Effects of ZnO, CuO and  $\gamma$ -Fe<sub>3</sub>O<sub>4</sub> nanoparticles on mature embryo culture of wheat (*Triticum aestivum* L.). *Plant Cell Tissue Organ Cult. (PCTOC)* **2019**, *136*, 269–277. [[CrossRef](#)]
- Türkoğlu, A.; Haliloğlu, K.; Demirel, F.; Aydın, M.; Çiçek, S.; Yiğider, E.; Demirel, S.; Piekutowska, M.; Szulc, P.; Niedbała, G. Machine Learning Analysis of the Impact of Silver Nitrate and Silver Nanoparticles on Wheat (*Triticum aestivum* L.): Callus Induction, Plant Regeneration, and DNA Methylation. *Plants* **2023**, *12*, 4151. [[CrossRef](#)] [[PubMed](#)]
- Shin, S.W.; Song, I.H.; Um, S.H. Role of physicochemical properties in nanoparticle toxicity. *Nanomaterials* **2015**, *5*, 1351–1365. [[CrossRef](#)] [[PubMed](#)]
- Hafeez, A.; Razzaq, A.; Mahmood, T.; Jhanzab, H.M. Potential of copper nanoparticles to increase growth and yield of wheat. *J. Nanosci. Adv. Technol.* **2015**, *1*, 6–11.
- Burger, A.; Lichtscheidl, I. Strontium in the environment: Review about reactions of plants towards stable and radioactive strontium isotopes. *Sci. Total Environ.* **2019**, *653*, 1458–1512. [[CrossRef](#)] [[PubMed](#)]
- Bronner, F. Metals in bone: Aluminum, boron, cadmium, chromium, lanthanum, lead, silicon, and strontium. In *Principles of Bone Biology*; Elsevier: Amsterdam, The Netherlands, 2008; pp. 515–531.
- Brooks, R.R. *Geobotany and Biogeochemistry in Mineral Exploration*; Harper & Row: New York, NY, USA, 1972.
- Gupta, D.K.; Walther, C. *Behaviour of Strontium in Plants and the Environment*; Springer: Berlin/Heidelberg, Germany, 2018.
- Gungor, A.A.; Nadaroglu, H.; Gultekin, D.D. Synthesis and characterization of nano-strontium oxide (SrO) Using erzincan cimin grape (*Vitis vinifera*, Cimin). *Chem. Sci. Int. J.* **2019**, *26*, 1–7. [[CrossRef](#)]
- Nadaroglu, H.; Alaylı, A.; Ceker, S.; Ogutcu, H.; Agar, G. Biosynthesis of Silver nanoparticles and investigation of genotoxic effects and antimicrobial activity. *Int. J. Nano Dimens.* **2020**, *11*, 158–167.
- Nadaroglu, H.; Gungor, A.A.; Ince, S.; Babagil, A. Green synthesis and characterisation of platinum nanoparticles using quail egg yolk. *Spectrochim. Acta Part A Mol. Biomol. Spectrosc.* **2017**, *172*, 43–47. [[CrossRef](#)]
- Hoagland, D.R.; Arnon, D.I. The water-culture method for growing plants without soil. *Circular. Calif. Agric. Exp. Stn.* **1950**, *347*, 32.

24. Nezami, A.; Khazaei, H.R.; Boroumand, R.Z.; Hosseini, A. Effects of drought stress and defoliation on sunflower (*Helianthus annuus*) in controlled conditions. *Desert* **2008**, *12*, 99–104.
25. Lutts, S.; Kinet, J.; Bouharmont, J. NaCl-induced senescence in leaves of rice (*Oryza sativa* L.) cultivars differing in salinity resistance. *Ann. Bot.* **1996**, *78*, 389–398. [[CrossRef](#)]
26. Tiryaki, D.; Aydın, İ.; Atıcı, Ö. Psychrotolerant bacteria isolated from the leaf apoplast of cold-adapted wild plants improve the cold resistance of bean (*Phaseolus vulgaris* L.) under low temperature. *Cryobiology* **2019**, *86*, 111–119. [[CrossRef](#)] [[PubMed](#)]
27. Sahin, U.; Ekinci, M.; Ors, S.; Turan, M.; Yildiz, S.; Yildirim, E. Effects of individual and combined effects of salinity and drought on physiological, nutritional and biochemical properties of cabbage (*Brassica oleracea* var. capitata). *Sci. Hort.* **2018**, *240*, 196–204. [[CrossRef](#)]
28. Apsana, G.; George, P.; Devanna, N.; Yuvasravana, R. Biomimetic synthesis and antibacterial properties of strontium oxide nanoparticles using *Ocimum sanctum* leaf extract. *Asian J. Pharm. Clin. Res.* **2018**, *11*, 384–389.
29. Apsana, G.; George, P.; Devanna, N. Eco-Friendly Approach for the Efficient Biosynthesis of Mg<sub>3</sub>(PO<sub>4</sub>)<sub>2</sub> Nanoparticles Using Plant Extract of *Ocimum sanctum*. *Adv. Sci. Lett.* **2018**, *24*, 5514–5518. [[CrossRef](#)]
30. Alavi, M.A.; Morsali, A. Syntheses and characterization of Sr(OH)<sub>2</sub> and SrCO<sub>3</sub> nanostructures by ultrasonic method. *Ultrason. Sonochem.* **2010**, *17*, 132–138. [[CrossRef](#)]
31. Lee, Y.; Choi, J.-R.; Lee, K.J.; Stott, N.E.; Kim, D. Large-scale synthesis of copper nanoparticles by chemically controlled reduction for applications of inkjet-printed electronics. *Nanotechnology* **2008**, *19*, 415604. [[CrossRef](#)] [[PubMed](#)]
32. Dimkpa, C.O.; Latta, D.E.; McLean, J.E.; Britt, D.W.; Boyanov, M.I.; Anderson, A.J. Fate of CuO and ZnO nano- and microparticles in the plant environment. *Environ. Sci. Technol.* **2013**, *47*, 4734–4742. [[CrossRef](#)] [[PubMed](#)]
33. Jiang, F.; Shen, Y.; Ma, C.; Zhang, X.; Cao, W.; Rui, Y. Effects of TiO<sub>2</sub> nanoparticles on wheat (*Triticum aestivum* L.) seedlings cultivated under super-elevated and normal CO<sub>2</sub> conditions. *PLoS ONE* **2017**, *12*, e0178088. [[CrossRef](#)]
34. Iqbal, M.; Raja, N.I.; Mashwani, Z.-U.-R.; Hussain, M.; Ejaz, M.; Yasmeen, F. Effect of silver nanoparticles on growth of wheat under heat stress. *Iran. J. Sci. Technol. Trans. A Sci.* **2019**, *43*, 387–395. [[CrossRef](#)]
35. Rafique, R.; Arshad, M.; Khokhar, M.; Qazi, I.; Hamza, A.; Virk, N. Growth response of wheat to titania nanoparticles application. *NUST J. Eng. Sci.* **2014**, *7*, 42–46.
36. McManus, P.; Hortin, J.; Anderson, A.J.; Jacobson, A.R.; Britt, D.W.; Stewart, J.; McLean, J.E. Rhizosphere interactions between copper oxide nanoparticles and wheat root exudates in a sand matrix: Influences on copper bioavailability and uptake. *Environ. Toxicol. Chem.* **2018**, *37*, 2619–2632. [[CrossRef](#)]
37. Mahmoodzadeh, H.; Ebadi, M.; Baharara, J. Effects of titanium dioxide nanoparticles (TiO<sub>2</sub>) on germination and seedling growth of Vitex plants (*Vitex agnus-castus* L.). *J. BioSci. Biotech.* **2019**, *8*, 141–149.
38. Zengin, F.K.; Munzuroglu, O. Effects of some heavy metals on content of chlorophyll, proline and some antioxidant chemicals in bean (*Phaseolus vulgaris* L.) seedlings. *Acta Biol. Cracoviensia Ser. Bot.* **2005**, *47*, 157–164.
39. Demir, N. Determination of Some Bioactivities and Chemical Composition of Tulip (*Tulipa armena*) Plant and Investigation of Usability as Homeopathic Drugs. *Int. J. Innov. Res. Rev.* **2018**, *2*, 21–23.
40. Ali, S.; Rizwan, M.; Hussain, A.; ur Rehman, M.Z.; Ali, B.; Yousaf, B.; Wijaya, L.; Alyemeni, M.N.; Ahmad, P. Silicon nanoparticles enhanced the growth and reduced the cadmium accumulation in grains of wheat (*Triticum aestivum* L.). *Plant Physiol. Biochem.* **2019**, *140*, 1–8. [[CrossRef](#)] [[PubMed](#)]
41. Hussain, A.; Rizwan, M.; Ali, Q.; Ali, S. Seed priming with silicon nanoparticles improved the biomass and yield while reduced the oxidative stress and cadmium concentration in wheat grains. *Environ. Sci. Pollut. Res.* **2019**, *26*, 7579–7588. [[CrossRef](#)]
42. Yuce, M.; Taspinar, M.S.; Aydin, M.; Agar, G. Response of NAC transcription factor genes against chromium stress in sunflower (*Helianthus annuus* L.). *Plant Cell Tissue Organ Cult. (PCTOC)* **2019**, *136*, 479–487. [[CrossRef](#)]
43. Cao, X.; Ma, C.; Chen, F.; Luo, X.; Musante, C.; White, J.C.; Zhao, X.; Wang, Z.; Xing, B. New insight into the mechanism of graphene oxide-enhanced phytotoxicity of arsenic species. *J. Hazard. Mater.* **2021**, *410*, 124959. [[CrossRef](#)]
44. Iftikhar, A.; Ali, S.; Yasmeen, T.; Arif, M.S.; Zubair, M.; Rizwan, M.; Alhathloul, H.A.S.; Alayafi, A.A.; Soliman, M.H. Effect of gibberellic acid on growth, photosynthesis and antioxidant defense system of wheat under zinc oxide nanoparticle stress. *Environ. Pollut.* **2019**, *254*, 113109. [[CrossRef](#)]
45. Tozlu, E.; Mohammadi, P.; Kotan, M.S.; Nadaroglu, H.; Kotan, R. Biological control of *Sclerotinia sclerotiorum* (Lib.) de Bary, the causal agent of white mould disease in red cabbage, by some bacteria. *Plant Prot. Sci.* **2016**, *52*, 188–198. [[CrossRef](#)]
46. Kheiri, A.; Jorf, S.M.; Malhipour, A.; Saremi, H.; Nikkhab, M. Application of chitosan and chitosan nanoparticles for the control of Fusarium head blight of wheat (*Fusarium graminearum*) in vitro and greenhouse. *Int. J. Biol. Macromol.* **2016**, *93*, 1261–1272. [[CrossRef](#)] [[PubMed](#)]
47. Rafique, R.; Zahra, Z.; Virk, N.; Shahid, M.; Pinelli, E.; Park, T.J.; Kallerhoff, J.; Arshad, M. Dose-dependent physiological responses of *Triticum aestivum* L. to soil applied TiO<sub>2</sub> nanoparticles: Alterations in chlorophyll content, H<sub>2</sub>O<sub>2</sub> production, and genotoxicity. *Agric. Ecosyst. Environ.* **2018**, *255*, 95–101. [[CrossRef](#)]
48. Saleh, A.M.; Hassan, Y.M.; Selim, S.; AbdElgawad, H. NiO-nanoparticles induce reduced phytotoxic hazards in wheat (*Triticum aestivum* L.) grown under future climate CO<sub>2</sub>. *Chemosphere* **2019**, *220*, 1047–1057. [[CrossRef](#)]
49. Chen, J.; Liu, X.; Wang, C.; Yin, S.-S.; Li, X.-L.; Hu, W.-J.; Simon, M.; Shen, Z.-J.; Xiao, Q.; Chu, C.-C. Nitric oxide ameliorates zinc oxide nanoparticles-induced phytotoxicity in rice seedlings. *J. Hazard. Mater.* **2015**, *297*, 173–182.

50. Da Costa, M.; Sharma, P. Effect of copper oxide nanoparticles on growth, morphology, photosynthesis, and antioxidant response in *Oryza sativa*. *Photosynthetica* **2016**, *54*, 110–119. [[CrossRef](#)]
51. García-Gómez, C.; García, S.; Obrador, A.F.; González, D.; Babín, M.; Fernández, M.D. Effects of aged ZnO NPs and soil type on Zn availability, accumulation and toxicity to pea and beet in a greenhouse experiment. *Ecotoxicol. Environ. Saf.* **2018**, *160*, 222–230. [[CrossRef](#)]
52. Büyük, İ.; Soydam Aydın, S.; Aras, E. Molecular responses of plants to stress conditions. *Turk. Bull. Hyg. Exp. Biol.* **2012**, *69*, 97–110.
53. Büyük, M.; İnci, M.; Tan, A.; Tümay, M. Improved instantaneous power theory based current harmonic extraction for unbalanced electrical grid conditions. *Electr. Power Syst. Res.* **2019**, *177*, 106014. [[CrossRef](#)]
54. Du, W.; Gardea-Torresdey, J.L.; Ji, R.; Yin, Y.; Zhu, J.; Peralta-Videa, J.R.; Guo, H. Physiological and biochemical changes imposed by CeO<sub>2</sub> nanoparticles on wheat: A life cycle field study. *Environ. Sci. Technol.* **2015**, *49*, 11884–11893. [[CrossRef](#)]
55. Jhanzab, H.M.; Razzaq, A.; Bibi, Y.; Yasmeen, F.; Yamaguchi, H.; Hitachi, K.; Tsuchida, K.; Komatsu, S. Proteomic analysis of the effect of inorganic and organic chemicals on silver nanoparticles in wheat. *Int. J. Mol. Sci.* **2019**, *20*, 825. [[CrossRef](#)] [[PubMed](#)]

**Disclaimer/Publisher's Note:** The statements, opinions and data contained in all publications are solely those of the individual author(s) and contributor(s) and not of MDPI and/or the editor(s). MDPI and/or the editor(s) disclaim responsibility for any injury to people or property resulting from any ideas, methods, instructions or products referred to in the content.